Letters

Research on a Time-Variant Shoot-Through Modulation Strategy for Quasi-Z-Source Inverter

Yufei Zhou, *Member, IEEE*, Qibin Wu, Zikai Li, and Feng Hong

***Abstract*—This letter proposes a time-variant shoot-through pulsewidth modulation strategy for the traditional modulation techniques used in quasi-Z-source inverters. By introducing the proposed strategy into the traditional modulation techniques, like the simple boost modulation, the bus voltage amplitude can be reduced at the nonpeak areas, and the switching loss can be greatly saved to improve system efficiency. Because the output voltage gain can still be guaranteed, the waveform quality is not influenced. At the same time, for the traditional zero states in the proposed strategy are fully used as the shoot-through zero states, the switching times can be evidently reduced and the system efficiency can be further increased. Theoretical analysis and experimental results are presented to verify the real performance.**

***Index Terms*—Efficiency, pulsewidth modulation (PWM), quasi-z-source inverter (qZSI), shoot-through zero state.**

I. Introduction

RENEWABLE energy resources such as solar and wind energy often experience large output voltage change, due to the fluctuation of the surrounding environment conditions [1]. This brings a great challenge to the inverter topology and control. Instead of the traditional buck-type voltage-source inverter (VSI) [2], [3], a two-stage circuit structure with a boost dc–dc converter added in front of the three-phase inverter bridge is usually adopted [4], [5]. When the input voltage is at a low level, the dc–dc converter can boost it to the required value and make the design and control of the down-stream inverter much easier. However, the two-stage solution has some inherent drawbacks. The dc–dc stage has serious reverse-recovery problem, especially under large duty cycle operation condition that deteriorates system efficiency. Moreover, the VSI bridge has shoot-through issue and needs dead time inserted between the drive signals of the switches on the same leg to avoid bridge shooting through. Dead time greatly improves system reliability but also causes waveform distortion of the output voltage [6]–[8], and still cannot totally eliminate bridge shoot-through especially under strong electromagnetic interference environment.

Manuscript received December 22, 2017; revised January 28, 2018 and February 26, 2018; accepted March 7, 2018. Date of publication March 14, 2018; date of current version August 7, 2018. This work was supported in part by the National Nature Science Foundation of China under Grant 51407089, in part by Aeronautical Science Foundation of China under Grant 2015ZC52035, in part by China Postdoctoral Science Foundation under Grant 2015M580424, in part by Foundation of Graduate Innovation Center in NUAA No. kfjj20160403, and in part by Fundamental Research Funds for the Central Universities. *(Corresponding author: Yufei Zhou.)*

The authors are with the College of Electronic and Information Engineering, Nanjing University of Aeronautics and Astronautics, Nanjing 211100, China (e-mail:

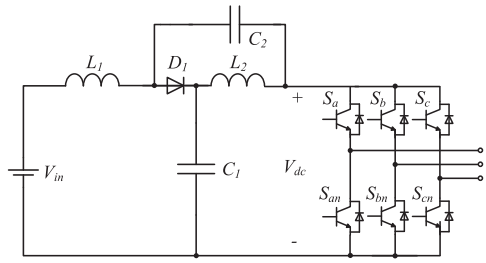

Fig. 1. Quasi-ZSI.

Z-source inverter (ZSI) [9] and quasi-ZSIs (qZSIs) [10] have been widely studied in recent years. They introduce a simple impedance network without active switches in front of the inverter bridge, and use bridge shooting through as a control variable to regulate magnitude of the dc-bus voltage, and then transfer energy to the load during active states. The qZSIs are proposed to improve the performance of ZSI and have similar operation principle and control strategy. One typical circuit configuration of qZSI is shown in Fig. 1.

The PWM technique applied has great impact on the performance of qZSIs. Several modulation techniques can be found in literatures with different characteristics and performance [9], [11]–[15].The simple boost PWM (SB PWM) proposed in [9] is simple and features with small current stress of switching devices. The main drawback of this method is its limitation on the shoot-through duty cycle. The six-section-distribution PWM method proposed in [9] divides the shoot-through time intervals into six sections in one switching cycle and distributing them into the traditional zero state without causing extra switching times. The maximum boost PWM proposed in [11] fully utilizes the traditional zero state as shoot-through zero state and greatly reduces the bus voltage. But it results in low frequency current ripple. The maximum constant boost PWM is proposed in [12]. Compared with the SB PWM, the bus voltage is lower and remains constant when the output voltage gain is the same. A hybrid switching method by combining PWM

with pulse amplitude modulation is proposed in [13]. It operates the switching devices in fundamental frequency, and is only applicable to single-phase qZSI system. In [14], a strategy that replaces the triangular wave carrier in PWM with the sine wave carrier is proposed. Higher boost capability can be obtained and the output voltage total harmonic distortion (THD) can be reduced. A double switching frequency PWM that utilizes high-frequency PWM with low-frequency SPWM is proposed in [15]. The converter can be designed more compact and operate with lower switching loss. The single-phase PWM method proposed in [16] and the pulsewidth-amplitude modulation proposed in [17] reduce the switching frequency compared to traditional three-phase PWM method, leading to less switching loss. These shoot-through PWM techniques try to improve system performance, but still have limitations.

This letter proposes a time-variant shoot-through PWM (TVST PWM) strategy for qZSI, which can improve the performance of the traditional modulation techniques. The shoot through duty cycle of the proposed modulation method changes as the output ac voltage changes across the whole cycle, and reaches its maximum value only at the peak of the ac output voltage. In this way, the shoot-through duty cycle at the non-peak areas can be reduced, leading to smaller switching loss of the inverter bridge and increasing system efficiency. Because the voltage gain can be guaranteed across the whole output ac cycle, the waveform quality will not be influenced. Furthermore, the modulation index and the shoot through duty cycle can be adjusted properly and then some traditional zero states can be fully utilized as shoot through zero states that helps to reduce switching times, leading to further increased system efficiency. For simplicity, this letter only analyzes the TVST PWM strategy based on the SB PWM technique [9].

II. Proposed TVST PWM for QZSI

A. Principle of qZSI

Fig. 1 shows the discussed qZSI in which inductors L_1 and L_2, capacitors C_1 and C_2, and diode D_1 construct an impedance network. By inserting shoot-through into the drive signals, the input voltage V_{in} can be stepped up to the desired dc-bus voltage V_{dc}. The dc-bus voltage can be expressed as

$$V_{\text{dc}} = \frac{1}{1-2D_0} V_{\text{in}} \tag{1}$$

where D_0 is the shoot-through duty cycle.

The relationship between the instantaneous output three-phase voltage and the dc-bus voltage can be derived from [18], and can be expressed as

$$\begin{cases} v_{\text{a}} = V_{\text{dc}} \frac{m_{\text{a}}}{2} \\ v_{\text{b}} = V_{\text{dc}} \frac{m_{\text{b}}}{2} \\ v_{\text{c}} = V_{\text{dc}} \frac{m_{\text{c}}}{2} \end{cases} \tag{2}$$

where m_a, m_b, m_c are the instantaneous modulation index. The waveforms of v_{a}, v_{b}, v_{c} are shown in Fig. 2.

As can be seen from (2), the output voltage can be adjusted by the dc-bus voltage and the instantaneous modulation index. The

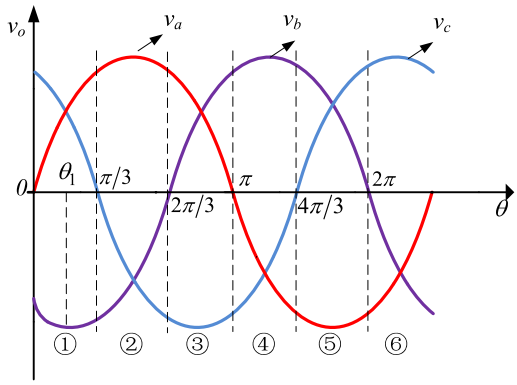

Fig. 2. Waveforms of the three-phase output voltage.

three-phase instantaneous modulation index can be expressed as

$$\begin{cases} m_a = M \sin\theta \\ m_b = M \sin\left(\theta - \frac{2\pi}{3}\right) \\ m_c = M \sin\left(\theta + \frac{2\pi}{3}\right) \end{cases} \tag{3}$$

where M is the modulation index.

B. Mechanism of TVST PWM

The traditional shoot-through modulation techniques, such as the SB PWM, insert a constant shoot-through zero state into the traditional zero state to step up the dc-bus voltage to a constant value, which can satisfy the peak gain requirement of the three-phase output sinusoidal voltage. Take the SB PWM technique as an example, which is shown in Fig. 3(a), the constant shoot-through duty cycle D_0 is obtained by comparing the shoot-through references $V_p = 1 - D_0$ and $V_n = D_0 - 1$ to the triangular carrier. Because of the constant shoot-through duty cycle D_0, the magnitude of the dc-bus voltage V_{dc} is also constant. The relationship between the magnitude of the output ac voltage and the dc-bus voltage is $V_{\text{om}} = (M/2)V_{\text{dc}}$, and also according to $M + D_0 = 1$ [19], we can get

$$V_{\text{dc}} = (2G - 1)\, V_{\text{in}} \tag{4}$$

where the output voltage gain $G = 2V_{\text{om}}/V_{\text{in}}$. From (4), the dc-bus voltage is determined by the input voltage and the output voltage gain. The relationship between the three-phase output voltage and the dc-bus voltage meets (2).

The inserting of the shoot-through zero state increases not only switching times of the inverter bridge, but also the magnitude of the dc-bus voltage, leading to additional switching loss and lower efficiency. Therefore, less or even no shoot-through zero state is preferred under low output voltage gain conditions. As indicated from Fig. 2, the shoot-through duty cycle under the nonpeak areas of the output phase voltage can be decreased to reduce the magnitude of the dc-bus voltage, on the precondition of satisfying the instantaneous output voltage gain.

The TVST PWM based on the SB PWM technique is shown in Fig. 3(b). The output sinusoidal cycle is divided into six sections equally. In each section, only one phase of the output voltage has the currently biggest absolute voltage value. Take section $(0, \pi/3)$ as an example, phase B has the biggest absolute

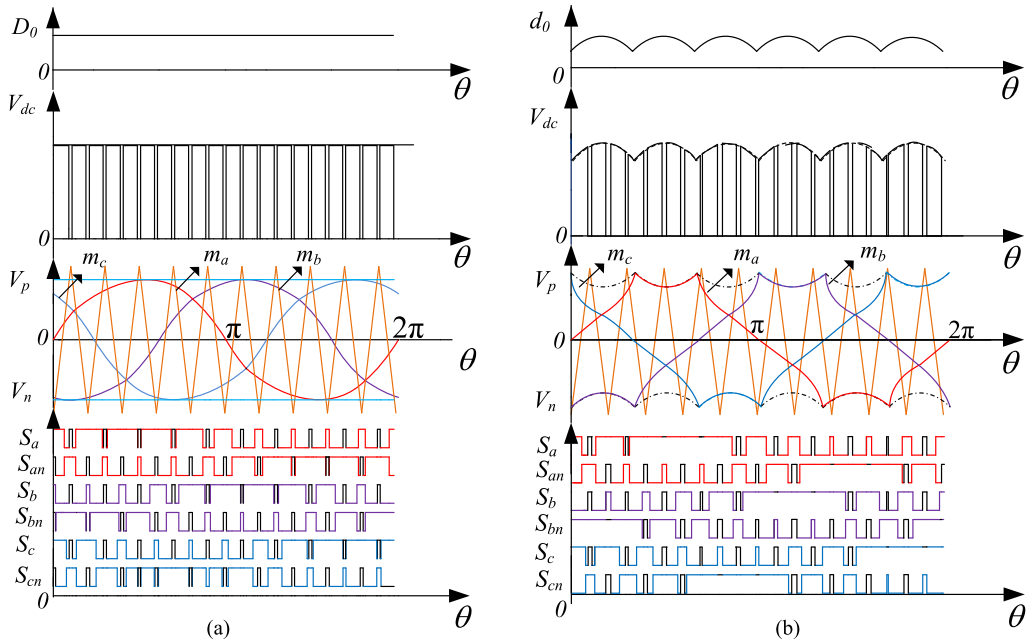

Fig. 3. Shoot-through duty cycle, dc-bus voltage, three-phase instantaneous modulation index, driving signals of (a) SB PWM and (b) TVST PWM.

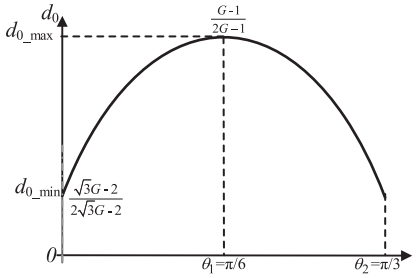

Fig. 4. Function curve of the shoot-through duty cycle in section (0, π/3).

voltage value, which can be expressed as

$$v_b(\theta) = V_{\mathrm{om}} \sin\left(\theta - \frac{2\pi}{3}\right). \tag{5}$$

According to $M + D_0 = 1$, (1), and (2), the shoot-through duty cycle of section (0, π/3) can be obtained as

$$d_0(\theta) = \frac{G\sin\left(\theta - \frac{2\pi}{3}\right) + 1}{2G\sin\left(\theta - \frac{2\pi}{3}\right) + 1}. \tag{6}$$

According to (6), the function curve of the shoot-through duty cycle $d_0(\theta)$ in section (0, π/3) is shown in Fig. 4. In this section, the maximum shoot-through duty cycle $d_{0\_\max}$ equals to $(G-1)/(2G-1)$ at the peak of phase B voltage with $\theta = \theta_1$. Meanwhile, the minimum shoot-through duty cycle $d_{0\_\min}$ equals to $(\sqrt{3}G-2)/(2\sqrt{3}G-2)$ at $\theta = 0$ or $\theta = \theta_2$. It can be seen that the shoot-through zero state at the nonpeak areas of the output voltage is decreased, which improved the corresponding instantaneous modulation index. The desired shoot-through duty cycle of the other five sections can also be derived, as shown in Table I.

By substituting (6) into (1), the dc-bus voltage of section (0, π/3) can be expressed as

$$v_{\mathrm{dc}}(\theta) = \frac{V_{\mathrm{in}}}{1 - 2d_0(\theta)} = \left(\left|2G\sin\left(\theta - \frac{2\pi}{3}\right)\right| - 1\right) V_{\mathrm{in}}. \tag{7}$$

The dc-bus voltage of the other five sections can also be derived, as shown in Table 1. The envelope line of the dc-bus voltage fluctuates with ripples of six times of the output frequency, as shown in Fig. 3(b). According to (1) and (2), the instantaneous modulation index of the output three-phase voltage can be derived as

$$\begin{cases} m_a(\theta) = G(1-2d_0)\sin(\theta) \\ m_b(\theta) = G(1-2d_0)\sin\left(\theta - \frac{2\pi}{3}\right) \\ m_c(\theta) = G(1-2d_0)\sin\left(\theta + \frac{2\pi}{3}\right) \end{cases}. \tag{8}$$

The function curves are shown in Fig. 3(b). The instantaneous modulation index of the other five sections can also be derived, as shown in Table I. The characteristics of the TVST PWM can be summarized as follows.

1) Compared to the SBPWM, the instantaneous voltage gain at the nonpeak areas of the output ac voltage can be reduced by using smaller shoot-through zero states inserted, and the dc-bus voltage amplitude can be lowered accordingly, leading to smaller switching loss and higher system efficiency.
2) To reduce the shoot through duty cycle and increase the instantaneous modulation index to the most when providing enough voltage gain, the maximum limit between the shoot-through duty cycle and the instantaneous modulation index can be taken, which is $d_0 + m = 1$. In this way, the shoot through reference $V_{\mathrm{p}} = 1 - d_0$ and $V_{\mathrm{n}} = d_0 - 1$ coincide with the curve of the modulation index for the phase voltage with maximum instantaneous value. And

TABLE I
DC-BUS VOLTAGE, SHOOT-THROUGH DUTY CYCLE AND INSTANTANEOUS MODULATION INDEX IN DIFFERENT SECTIONS OF THE OUTPUT SINUSOIDAL CYCLE

θ	Maximum output phase voltage	DC-bus voltage	$d_0(\theta)$	$m_a(\theta)$	$m_{\rm b}(\theta)$	$m_{\rm c}(\theta)$
$0 \sim \frac{\pi}{3}$	v_b	$\left(\left\|2G\sin\left(\theta-\frac{2\pi}{3}\right)\right\|-1\right)V_{\rm in}$	$\frac{G\sin\left(\theta-\frac{2\pi}{3}\right)+1}{2G\sin\left(\theta-\frac{2\pi}{3}\right)+1}$	$\frac{-G\sin(\theta)}{2G\sin\left(\theta-\frac{2\pi}{3}\right)+1}$	$\frac{-G\sin\left(\theta-\frac{2\pi}{3}\right)}{2G\sin\left(\theta-\frac{2\pi}{3}\right)+1}$	$\frac{-G\sin\left(\theta+\frac{2\pi}{3}\right)}{2G\sin\left(\theta-\frac{2\pi}{3}\right)+1}$
$\frac{\pi}{3} \sim \frac{2\pi}{3}$	v_a	$(\|2G\sin(\theta)\|-1)V_{\rm in}$	$\frac{G\sin(\theta)-1}{2G\sin(\theta)-1}$	$\frac{G\sin(\theta)}{2G\sin(\theta)-1}$	$\frac{G\sin\left(\theta-\frac{2\pi}{3}\right)}{2G\sin(\theta)-1}$	$\frac{G\sin\left(\theta+\frac{2\pi}{3}\right)}{2G\sin(\theta)-1}$
$\frac{2\pi}{3} \sim \pi$	v_c	$\left(\left\|2G\sin(\theta+\frac{2\pi}{3})\right\|-1\right)V_{\rm in}$	$\frac{G\sin\left(\theta+\frac{2\pi}{3}\right)+1}{2G\sin\left(\theta+\frac{2\pi}{3}\right)+1}$	$\frac{-G\sin(\theta)}{2G\sin\left(\theta+\frac{2\pi}{3}\right)+1}$	$\frac{-G\sin\left(\theta-\frac{2\pi}{3}\right)}{2G\sin\left(\theta+\frac{2\pi}{3}\right)+1}$	$\frac{-G\sin\left(\theta+\frac{2\pi}{3}\right)}{2G\sin\left(\theta+\frac{2\pi}{3}\right)+1}$
$\pi \sim \frac{4\pi}{3}$	v_b	$\left(\left\|2G\sin\left(\theta-\frac{2\pi}{3}\right)\right\|-1\right)V_{\rm in}$	$\frac{G\sin\left(\theta-\frac{2\pi}{3}\right)-1}{2G\sin\left(\theta-\frac{2\pi}{3}\right)-1}$	$\frac{G\sin(\theta)}{2G\sin\left(\theta-\frac{2\pi}{3}\right)-1}$	$\frac{G\sin\left(\theta-\frac{2\pi}{3}\right)}{2G\sin\left(\theta-\frac{2\pi}{3}\right)-1}$	$\frac{G\sin\left(\theta+\frac{2\pi}{3}\right)}{2G\sin\left(\theta-\frac{2\pi}{3}\right)-1}$
$\frac{4\pi}{3} \sim \frac{5\pi}{3}$	v_a	$(\|2G\sin(\theta)\|-1)V_{\rm in}$	$\frac{G\sin(\theta)+1}{2G\sin(\theta)+1}$	$\frac{-G\sin(\theta)}{2G\sin(\theta)+1}$	$\frac{-G\sin\left(\theta-\frac{2\pi}{3}\right)}{2G\sin(\theta)+1}$	$\frac{-G\sin\left(\theta+\frac{2\pi}{3}\right)}{2G\sin(\theta)+1}$
$\frac{5\pi}{3} \sim 2\pi$	v_c	$\left(\left\|2G\sin\left(\theta+\frac{2\pi}{3}\right)\right\|-1\right)V_{\rm in}$	$\frac{G\sin\left(\theta+\frac{2\pi}{3}\right)-1}{2G\sin\left(\theta+\frac{2\pi}{3}\right)-1}$	$\frac{G\sin(\theta)}{2G\sin\left(\theta+\frac{2\pi}{3}\right)-1}$	$\frac{G\sin\left(\theta-\frac{2\pi}{3}\right)}{2G\sin\left(\theta+\frac{2\pi}{3}\right)-1}$	$\frac{G\sin\left(\theta+\frac{2\pi}{3}\right)}{2G\sin\left(\theta+\frac{2\pi}{3}\right)-1}$

then the traditional zero state is fully utilized by the shoot-through zero state, as shown in Fig. 3(b). This greatly reduces the switching times and increases system efficiency.

III. LOSS ANALYSIS

Loss of quasi-ZSI mainly comes from the three-phase inverter bridge and the passive network. Loss of the inverter bridge includes conduction loss $P_{\rm con\_IGBT}$ and switching loss $P_{\rm sw\_IGBT}$ of the switches, conduction loss $P_{{\rm con\_}D{\rm \_para}}$ and turn-OFF loss $P_{\rm sw\_D\_para}$ of the antiparalleled diodes. Loss of the impedance network can be divided into winding loss and core loss of the inductors P_{L_z}, conduction loss $P_{{\rm con\_}D1}$, and reverse recovery related loss $P_{{\rm rr\_}D1}$ of the diode. The capacitors of the impedance network are generally of film type, and the loss P_{C_z} generated is negligible because the equivalent series resistance is very small. The calculation of power loss is similar to qZSI with traditional modulation techniques. Due to the paper length, the detailed calculation process is neglected, and the calculated power losses of each device are shown in Fig. 5, based on the same operating conditions and parameters as shown in Section IV.

By using the TVST PWM, the shoot through duty cycle at the nonpeak areas can be reduced, and the conduction loss during the shoot through zero state can be saved. The switching loss of the IGBTs, the turn-OFF loss of the antiparalleled diode, and the reverse recovery loss of the diode in the impedance network can all be reduced for qZSI with TVST PWM, because the bus voltage at the nonpeak areas can be reduced, which is in direct proportion to the three part of loss. In addition, by using TVST PWM, the switching loss can be further reduced by the reduction of the switching times. Take switch S_a as an example, the traditional zero state is totally used by the shoot-through zero state within the domain of $\pi/3 \sim 2\pi/3$, so the switching times can be reduced by 1/3. The turn-OFF loss of the antiparalleled diode can also reduced by the reduction of the switching times.

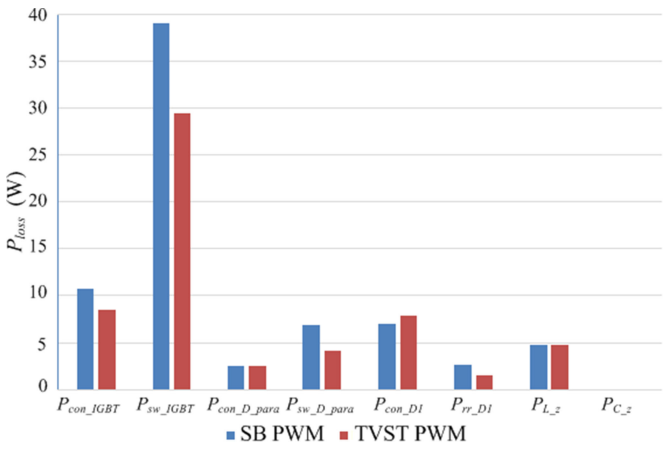

Fig. 5. Power loss of qZSI with SB PWM and TVST PWM.

IV. EXPERIMENTAL VERIFICATION

A 1000-VA prototype of quasi-ZSI shown in Fig. 1 was built to verify the performance of the proposed TVST PWM strategy. The carrier frequency is 10 KHz. The inductance of L_1 and L_2 are both 3 mH. The capacitance of C_1 and C_2 are both 2 μF. The output three-phase *LC* filter is configured with inductance of 8.5 mH and capacitance of 9.4 uF. MUR30120 is used as the diode in the impedance network, and PS21A79 from Mitsubishi is used as the inverter bridge. The input voltage is 240 V, and the output phase voltage with amplitude of 156 V and frequency of 50 Hz. The load applied on the output is 36.3 Ω. The experimental results of the TVST PWM are shown in Fig. 6 with key

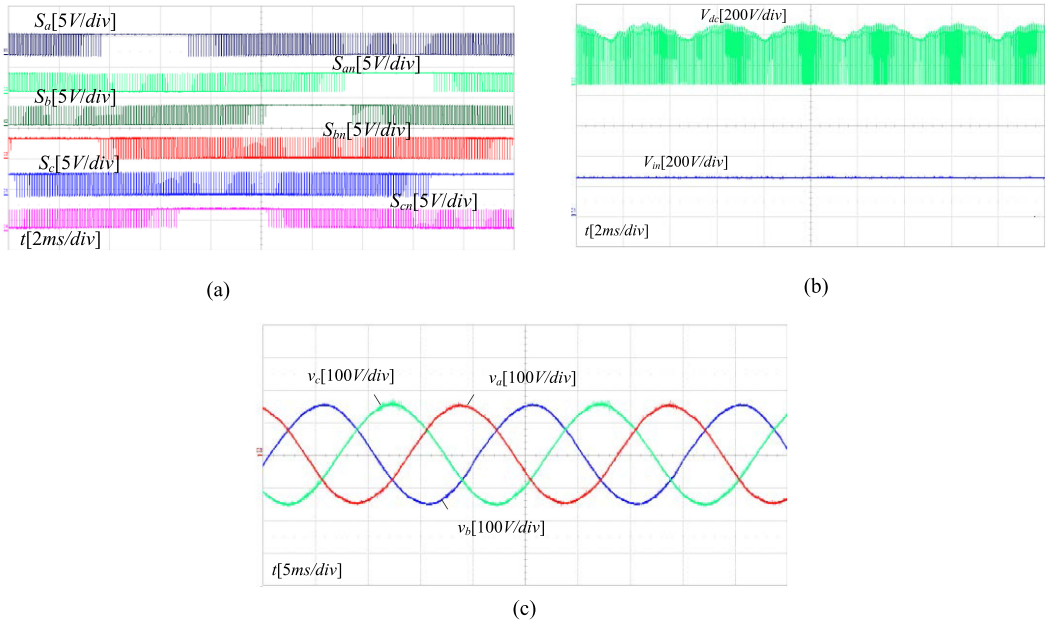

Fig. 6. Experimental results of TVST PWM. (a) Drive signals. (b) Bus voltage and input voltage. (c) Output three-phase voltage.

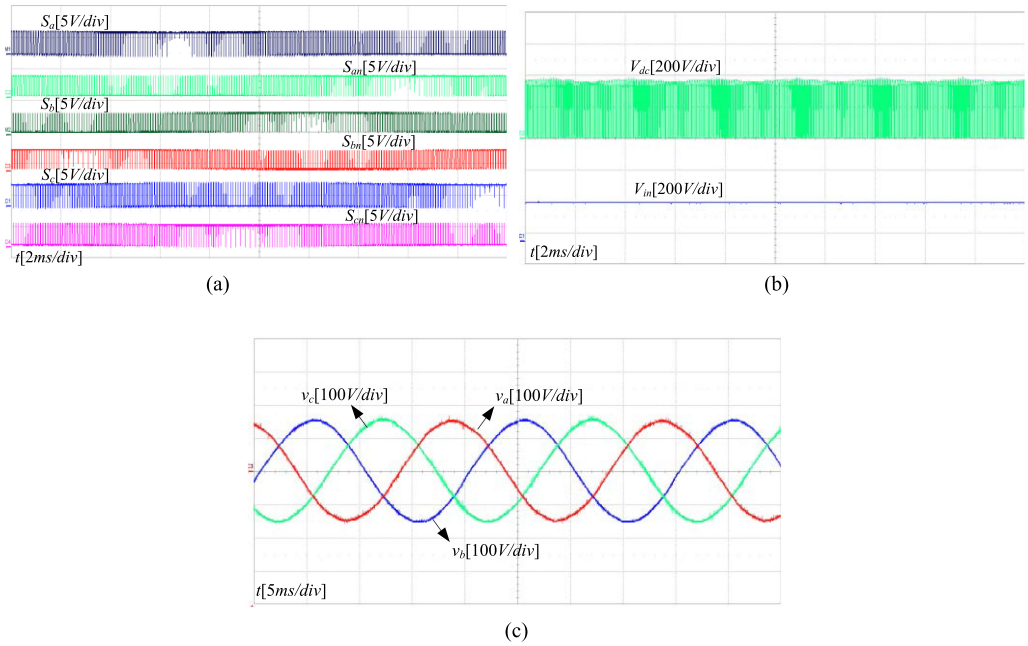

Fig. 7. Experimental results of SB PWM. (a) Drive signals. (b) Bus voltage and input voltage. (c) Output three-phase voltage.

operation waveforms. The drive signals waveform is shown in Fig. 6(a) with TVST duty cycle. Fig. 6(b) shows that the dc-bus voltage amplitude is also time-variant and the amplitude value at the nonpeak areas is much lower than that of the constant shoot through modulation strategies, which indicates higher conversion efficiency. As can be seen from Fig. 6(c), although the envelope of the dc-bus voltage fluctuates with ripples, the waveforms of the modulated three-phase output voltage are smooth and sinusoidal, which indicates small distortion. This is because the voltage gain of the proposed TVST PWM strategy can still be guaranteed. The tested THD was 1.05%.

For comparison purpose, a prototype based on the SB modulation technique is tested with the same circuit configuration, parameters, and test conditions. The D_0 is a constant value of 0.186, and M equals to 0.814. The experimental results are shown in Fig. 7 with constant shoot-through duty cycle, constant bus voltage amplitude. The bus voltage amplitude is 395 V. Fig. 7(c) shows the output three-phase voltage amplitude with

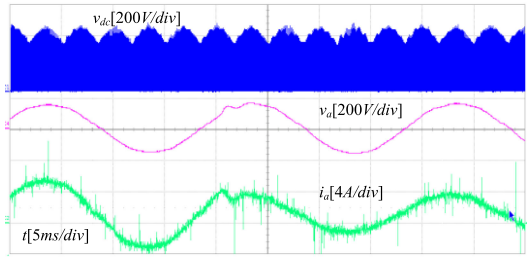

Fig. 8. Experimental results of the TVST PWM when load is changing.

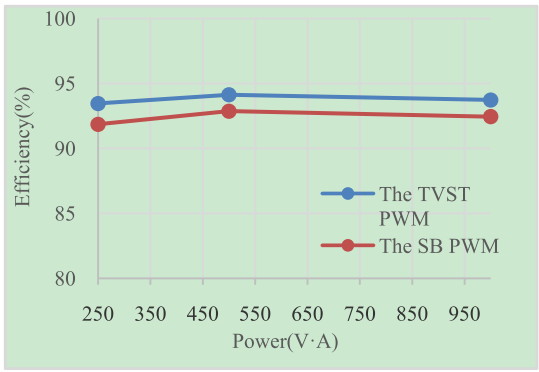

Fig. 9. Efficiency curve of the TVST PWM and the traditional SB PWM.

value of 156 V. The tested THD is 1.02%, measured by the harmonic analyzer. Fig. 8 shows the waveforms of output phase voltage v_a and current i_a, and dc-bus voltage $v_{\rm dc}$ when load changes from full load to half load. The envelope of dc-bus voltage and output phase voltage amplitude are stable when load is changing.

Fig. 9 gives an efficiency comparison between the converter with TVST PWM and with the traditional SB PWM. As can be seen, the efficiency improvement is evident by using the proposed TVST PWM strategy. The efficiency increase under light load conditions is more evident than under heavy load conditions. This is because the switching loss contributes more to the total loss under light load conditions. The tested efficiency of TVST PWM is 93.73% under full load of 1000 VA, 94.14% under half load, and 93.46% under one quarter load of TVST PWM, whereas the tested efficiency of traditional SB PWM is 92.44% under full load of 1000 VA, 92.87% under half load, and 91.86% under one quarter load.

V. Conclusion

In this letter, a TVST modulation strategy for qZSI is proposed. The proposed strategy can improve the traditional modulation techniques with increased system efficiency. Theoretical analysis and experimental results show that the use of the TVST modulation strategy can effectively reduce the bus voltage amplitude at the nonpeak areas of the ac output voltage and the switching loss can be reduced. Because the voltage gain can be guaranteed, waveform quality is not influenced. At the same time, for the traditional zero states are fully used as the shoot-through zero states, the switching times can also be reduced and the system efficiency can be further increased.

References

[1] B. M. Ge, F. Z. Peng, and H. Abu-Rub, "Novel energy stored single-stage photovoltaic power system with constant DC-link peak voltage," *IEEE Trans. Sustain. Energy*, vol. 5, no. 1, pp. 28–36, Jan. 2014.

[2] H. F. Bai, X. F. Wang, and C. L. Poh, "Harmonic analysis and mitigation of low-frequency switching voltage source inverter with series LC filtered VSI," in *Proc. IEEE Appl. Power Electron. Conf. Expo.*, Tampa, FL, USA, 2017, pp. 3299–3306.

[3] M. Mohebbi, M. L. McIntyre, and J. Latham, "A learning back stepping controller for voltage source inverter with nonlinear loads," in *Proc. IEEE Power Energy Conf. Illinois*, Champaign, IL, USA, 2017, pp. 1–5.

[4] T. Ding, C. Li, and Y. H. Yang, "A two-stage robust optimization for centralized-optimal dispatch of photovoltaic inverters in active distribution networks," *IEEE Trans. Sustain. Energy*, vol. 8, no 2, pp. 744–754, Apr. 2017.

[5] A. Morrison, J. W. Zapata, and S. Kouro, "Partial power DC-DC converter for photovoltaic two-stage string inverters," in *Proc. IEEE Energy Convers. Congr. Expo.*, Milwaukee, WI, USA, 2016, pp. 1–6.

[6] A. Mora, J. Juliet, and A. Santander, "Dead-time and semiconductor voltage drop compensation for cascaded H-bridge converters," *IEEE Trans. Ind. Electron.*, vol. 63, no. 12, pp. 7833–7842, Dec. 2016.

[7] U. Abronzini, C. Attaianese, M. D. Arpino, M. Di Monaco, V. Nardi, and G. Tomasso, "Dead time and nonlinearities compensation for VSI feeding AC drives," in *Proc. IEEE 26th Int. Symp. Ind. Electron.*, Edinburgh, U.K., 2017, pp. 271–276.

[8] C. Piao and J. Y. Hung, "Analysis and compensation of Dead-time effect in multi-level diode clamped VSI based on simplified SVPWM," in *Proc. IEEE 10th Conf. Ind. Electron. Appl.*, Auckland, New Zealand, 2015, pp. 375–380.

[9] F. Z. Peng, "Z-source inverter," *IEEE Trans. Ind. Appl.*, vol. 39, no. 2, pp. 504–510, Mar/Apr. 2003.

[10] J. Anderson and F. Z. Peng, "Four quasi-Z-Source inverters," in *Proc. IEEE Power Electr. Spec. Conf.*, Rhodes, Greece, 2008, pp. 2743–2749.

[11] F. Z. Peng, M. S. Shen, and Z. M. Qian, "Maximum boost control of the Z-source inverter," *IEEE Trans. Power Electron.*, vol. 20, no. 4, pp. 833–838, Jul. 2005.

[12] C. S. Singh and R. K. Tripathi, "Maximum constant boost control of switch inductor quasi Z-source inverter," in *Proc. Students Conf. Eng. Syst.*, Allahabad, India, 2013, pp. 1–5.

[13] Y. Liu, B. Ge, H. Abu-Rub, and H. Sun, "Hybrid pulse width modulated single-phase quasi-Z-source grid-tie photovoltaic power system," *IEEE Trans. Ind. Informat.*, vol. 12, no. 2, pp. 621–632, Apr. 2016.

[14] U. S. Ali, G. Brindha, A. H. Priya, and M. N. Karthikeyan, "A novel carrier based pulse width modulation technique for quasi-z-source inverter with improved voltage gain," in *Proc. Int. Conf. Circuits, Power Comput. Technol.*, Nagercoil, India, 2013, pp. 199–202.

[15] M. Mohammadi, J. S. Moghani, and J. Milimonfared, "A novel dual switching frequency modulation for Z-source and quasi Z-source inverters," *IEEE Trans. Ind. Electron.*, vol. 65, no. 6, pp. 5167–5176, Jun. 2018.

[16] H. Fujita, "A three-phase voltage-source solar power conditioner using a single-phase PWM control method," in *Proc. IEEE Energy Convers. Congr. Expo.*, 2009, pp. 3748–3754.

[17] Y. Li, Y. Liu, and H. Abu-Rub, "PWAM controlled quasi-Z source motor drive," in *Proc. IEEE 26th Int. Symp. Ind. Electron.*, Edinburgh, U.K., 2017, pp. 1669–1675.

[18] A. Ayad, M. Hashem, C. Hackl, and R. Kennel, "Proportional-resonant controller design for quasi-Z-source inverters with LC filters," in *Proc. 42nd Annu. Conf. IEEE Ind. Electron. Soc.*, Florence, Italy, 2016, pp. 3558–3563.

[19] P. K. Dhara, P. K. Gayen, and R. Garai, "Study on modeling & control of three phase quasi Z-source inverter for power conversion," in *Proc. 2016 Int. Conf. Comput., Elect. Commun. Eng.*, Kolkata, India, 2016, pp. 1–6.